



Kent Academic Repository

Haberichter, Mareike, MacKenzie, Richard, Paranjape, Manu and Ung, Yvan (2016) *Tunneling decay of false domain walls: the silence of the lambs*. *Journal of Mathematical Physics*, 57 (4). ISSN 0022-2488.

Downloaded from

<https://kar.kent.ac.uk/49091/> The University of Kent's Academic Repository KAR

The version of record is available from

<https://doi.org/10.1063/1.4947263>

This document version

Publisher pdf

DOI for this version

Licence for this version

UNSPECIFIED

Additional information

Versions of research works

Versions of Record

If this version is the version of record, it is the same as the published version available on the publisher's web site. Cite as the published version.

Author Accepted Manuscripts

If this document is identified as the Author Accepted Manuscript it is the version after peer review but before type setting, copy editing or publisher branding. Cite as Surname, Initial. (Year) 'Title of article'. To be published in *Title of Journal*, Volume and issue numbers [peer-reviewed accepted version]. Available at: DOI or URL (Accessed: date).

Enquiries

If you have questions about this document contact ResearchSupport@kent.ac.uk. Please include the URL of the record in KAR. If you believe that your, or a third party's rights have been compromised through this document please see our [Take Down policy](https://www.kent.ac.uk/guides/kar-the-kent-academic-repository#policies) (available from <https://www.kent.ac.uk/guides/kar-the-kent-academic-repository#policies>).

Tunneling decay of false domain walls: The silence of the lambs

Cite as: J. Math. Phys. 57, 042303 (2016); <https://doi.org/10.1063/1.4947263>

Submitted: 13 July 2015 . Accepted: 11 April 2016 . Published Online: 27 April 2016

Mareike Haberichter, Richard MacKenzie, M. B. Paranjape , and Yvan Ung



View Online



Export Citation



CrossMark

ARTICLES YOU MAY BE INTERESTED IN

[Classically Spinning Skyrmions](#)

AIP Conference Proceedings **1389**, 651 (2011); <https://doi.org/10.1063/1.3636815>

[Exactly solvable problems in the momentum space with a minimum uncertainty in position](#)

Journal of Mathematical Physics **57**, 042102 (2016); <https://doi.org/10.1063/1.4945313>

[Classically spinning and isospinning solitons](#)

AIP Conference Proceedings **1479**, 536 (2012); <https://doi.org/10.1063/1.4756186>



NEW

AVS Quantum Science

A high impact interdisciplinary journal for **ALL** quantum science

ACCEPTING SUBMISSIONS

Tunneling decay of false domain walls: The silence of the lambs

Mareike Haberichter,^{1,2,a)} Richard MacKenzie,^{3,b)} M. B. Paranjape,^{1,3,4,c)} and Yvan Ung^{3,d)}

¹*Department of Applied Mathematics and Theoretical Physics, University of Cambridge, Wilberforce Road, Cambridge CB3 0WA, United Kingdom*

²*School of Mathematics, Statistics and Actuarial Science, University of Kent, Canterbury CT2 7NF, United Kingdom*

³*Groupe de Physique des Particules, Département de Physique, Université de Montréal, C.P. 6128, Succursale Centre-ville, Montréal, Québec H3C 3J7, Canada*

⁴*St. John's College, University of Cambridge, Cambridge CB2 1TP, United Kingdom*

(Received 13 July 2015; accepted 11 April 2016; published online 27 April 2016)

We study the decay of “false” domain walls, that is, metastable states of the quantum theory where the true vacuum is trapped inside the wall with the false vacuum outside. We consider a theory with two scalar fields, a shepherd field and a field of sheep. The shepherd field serves to herd the solitons of the sheep field so that they are nicely bunched together. However, quantum tunnelling of the shepherd field releases the sheep to spread out uncontrollably. We show how to calculate the tunnelling amplitude for such a disintegration. *Published by AIP Publishing.* [<http://dx.doi.org/10.1063/1.4947263>]

I. INTRODUCTION

The notion of a vacuum in field theory is quite a bit richer than that in everyday language. In a theory with scalar fields, any state that is a local minimum of the potential energy density is a vacuum. More than one vacuum can exist, and not all vacua need to have the same energy. The lowest such state is called the true vacuum; any higher-energy local minimum is a false vacuum.

The most common reason for a multiplicity of vacua is spontaneous symmetry breaking. The breaking of a discrete symmetry gives rise to discrete vacua whereas the breaking of a continuous symmetry gives rise to a continuum of vacua. In this paper we restrict ourselves to discrete vacua. Depending on the model, a number (possibly infinite) of vacua of any energy can exist. Field configurations that interpolate between different degenerate vacua, true or false, give rise to domain walls (see, for example, Ref. 1) which themselves are stable or metastable. Domain walls are very important in cosmology^{1,2} and in condensed matter physics,³ where they quite often arise in the study of first-order phase transitions. A full review of domain walls and their applications is beyond the scope of this article, and we refer the reader to the cited literature.

In this paper we consider the special case of domain walls interpolating between distinct false vacua, with true vacuum in the core of the domain wall. The very existence of domain walls in our model is due to a subtle interplay between the energetics of two fields. The domain wall we consider entraps several quanta of a quantum field, ϕ , which we call the sheep field. These on their own would separate to infinity, leaving behind regions of true vacuum. It is the sheep field that is in the false vacuum outside the domain wall, but it is in regions passing through the true vacuum inside the domain wall. These sheep are herded into staying together, inside the domain wall, by a field we call the shepherd field, ψ . ψ is in its true vacuum outside the domain wall and in its false vacuum

a) M.Haberichter@kent.ac.uk

b) richard.mackenzie@umontreal.ca

c) paranj@lps.umontreal.ca

d) klignon_ecology@hotmail.com

inside the domain wall. The shepherd field is unstable to quantum tunnelling to its true vacuum; once this occurs, the sheep are without a shepherd and will spread out to infinity. We compute the amplitude for such a decay in a specific model analytically, aided by numerical calculations, within the collective coordinate approximation scheme. Thus, the sheep and shepherd field will be assumed to maintain fixed profiles while interacting and the locations of each domain wall in the system become the degrees of freedom. This approximation will provide an upper bound on the Euclidean action of the bounce and consequently a lower bound on the domain wall decay rate, as will be explained below. We have also studied an analogous model⁴ which shares some features of the model studied here; in particular, in the earlier work there are not multiple quanta of one field trapped inside the domain wall.

II. THE MODEL

Consider the model defined by the Lagrangian density

$$\mathcal{L} = \frac{1}{2} (\partial_\mu \psi \partial^\mu \psi + \partial_\mu \phi \partial^\mu \phi) - V(\psi, \phi), \quad (1)$$

where the potential is

$$V(\psi, \phi) = V_\psi(\psi) + V_\phi(\phi) + V_{\psi\phi}(\psi, \phi) - V_0 \quad (2)$$

with

$$V_\psi(\psi) = \beta(\psi + a)^2 \left((\psi - a)^2 + \epsilon_\psi^2 \right), \quad (3)$$

$$V_\phi(\phi) = \alpha \left(\sin^2(\pi\phi) + \epsilon_\phi \sin^2(\pi\phi/2) \right), \quad (4)$$

$$V_{\psi\phi}(\psi, \phi) = \lambda \frac{(\psi - a)^2 \left((\psi + a)^2 + \epsilon_\psi^2 \right)}{(V_\phi(\phi) - V_\phi(1/2))^2 + \gamma^2}. \quad (5)$$

λ is considered to be very small compared to β ; γ is considered small compared to $V_\phi(1/2)$. We impose that $V(\psi, \phi) \geq 0$. The first three terms are positive semi-definite, and then V_0 is chosen so that $V(\psi, \phi)$ vanishes at its global minimum. The ϕ field is essentially a sine-Gordon field (with alternating true and false vacua) while the ψ field has a rather standard double-well potential with a small asymmetry. Both fields admit kink-type solitons when $\epsilon_\phi = \epsilon_\psi = 0$. The interaction between the two fields is constructed to disallow the passage of the ϕ solitons through the ψ solitons. The specific potential that we use is not important; the only feature that is crucial is this “non-commutativity” of solitons, and any potential that achieves the result is adequate.

It is easy to see that the global minimum of V_ψ occurs at $\psi = -a$ while a local minimum occurs near $\psi = a$, as can be seen in Fig. 1. The minimum of $V_\phi(\phi)$ occurs at even integers $\phi = 2k$ with a slightly higher local minimum occurring at odd integers $\phi = 2k + 1$; degenerate local maxima occur at each half-odd integer, as can be seen in Fig. 2. The positions of these extrema are displaced by $V_{\psi\phi}(\psi, \phi)$, but by choosing λ small the displacements can be made arbitrarily small. Fig. 3 illustrates

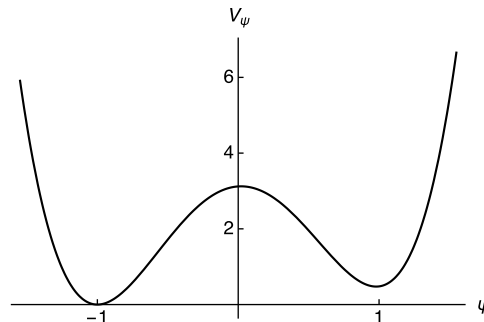


FIG. 1. The potential V_ψ for the field ψ with $a = 1$, $\beta = 3$, $\epsilon_\psi = 0.2$.

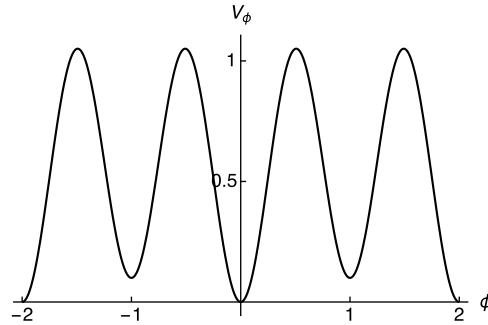


FIG. 2. The potential V_ϕ for the field ϕ with $\alpha = 1, \epsilon_\phi = 0.1$.

a three-dimensional plot of full potential (2) for a representative set of parameters. The potential is taken to be periodic in ϕ -direction.

Obviously for $\lambda = 0$, the true vacua correspond to $\{\psi = -a, \phi = 2k\}$ while $\{\psi = -a, \phi = 2k + 1\}$ or $\{\psi = a, \phi = 2k$ or $2k + 1\}$ correspond to the false vacua. Of course with λ non-zero, the values of the fields at the minima will be slightly modified, however the structure of the false and true vacua will remain unchanged. In the ensuing discussion, we will identify the vacua by the values that the fields take when $\lambda = 0$, but always with the understanding that the actual values that the fields take are slightly perturbed.

Since there are distinct vacua, we can imagine configurations corresponding to domain walls. Consider a domain wall interpolating between two false vacua $\phi = 2k + 1$ and $\phi = 2k' + 1$ with $\psi = -a$ remains at its true minimum. Such a domain wall passes through true vacua with ϕ even, so it is unstable, separating into several subsidiary domain walls. To be more concrete, consider the specific example where ϕ interpolates from $\phi = -1 \rightarrow \phi = 1$ with $\psi = -a$ (easily visualized in Fig. 3). Such a domain wall will be unstable, separating into two halves that interpolate from $\phi = -1 \rightarrow \phi = 0$ and then from $\phi = 0 \rightarrow \phi = 1$ while the ψ field remains always at $\psi = -a$. The intermediate region being the true vacuum, the two half-domain walls feel a repulsive force and will accelerate away from each other leaving behind them true vacuum.

However, we can construct metastable domain walls between the same false vacua (that is, domain walls that are classically stable but unstable via quantum tunnelling) by making a “detour” in field space. To see how this can be done (referring to Fig. 3), imagine a field configuration which consists of three branches (joined in some smooth manner), where, as x goes from minus to plus infinity, (ϕ, ψ) undergoes the sequence $(-1, -a) \rightarrow (-1, +a) \rightarrow (+1, +a) \rightarrow (+1, -a)$ thus encircling two of the “fins” of the full potential. The fields avoid the true vacuum $(\phi, \psi) = (0, -a)$ and so the

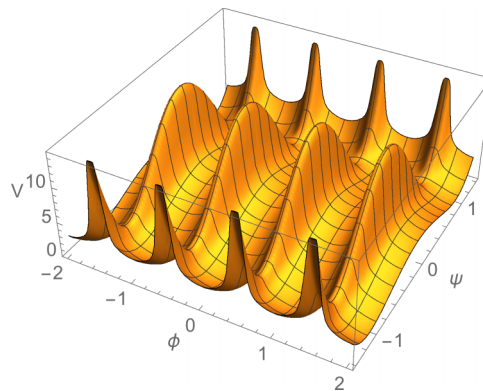


FIG. 3. 3d plot with $a = 1, \beta = 3, \epsilon_\phi = 0.2, \alpha = 1, \epsilon_\psi = 0.1, \lambda = 0.1, \gamma = 0.1$. Along the line $\psi = -1$, there are true minima at even values of ϕ and slightly higher-energy false vacua at odd values of ϕ . The situation is similar along the line $\psi = +1$, although all the vacua are raised in energy (so they are all false vacua) since $V_\psi(1) > 0$.

instability described above no longer applies. Furthermore, in order to “straighten” the soliton out in field space, the fields have to pass through the fins, which then provide a potential barrier preventing the straightening from occurring classically.

This field configuration can be described as a soliton of the ψ field followed by one of the ϕ fields and finally an anti-soliton of the ψ field. Fig. 4 illustrates just such a configuration, which is in fact a numerical solution of the following equations of motion:

$$\phi'' = 2\beta\pi\left(\sin(\pi\phi)\cos(\pi\phi) + \frac{\epsilon_\phi}{2}\sin(\pi\phi/2)\cos(\pi\phi/2)\right) + 2\lambda\left(V_\phi(\phi) - V_\phi(1/2)\right)\left(\beta\pi(\sin(2\pi\phi) + \frac{\epsilon_\phi}{2}\sin(\pi\phi))\right)\frac{(\psi - a)^2(\psi + a)^2 + \epsilon_\psi^2}{\left((V_\phi(\phi) - V_\phi(1/2))^2 + \gamma^2\right)^2}, \quad (6a)$$

$$\psi'' = 2\alpha(\psi + a)((\psi - a)^2 + \epsilon_\psi^2) - 2\alpha(\psi + a)^2(\psi - a) - 2\lambda\frac{(\psi - a)((\psi + a)^2 + \epsilon_\psi^2) + (\psi - a)^2(\psi + a)}{\left((V_\phi(\phi) - V_\phi(1/2))^2 + \gamma^2\right)}, \quad (6b)$$

where the prime denotes differentiation with respect to the spatial coordinate. Eqs. (6) were solved using the gradient flow method⁵ with the boundary conditions chosen as stated above. Note that the same parameter values were used throughout the rest of the paper.

In the stability analysis, the interaction term makes the following crucial contribution. The point is that if ϕ passes through the value $1/2$ when ψ is such that the numerator in the interaction term is not very small or zero (this means that $\psi \neq \pm a$), then the denominator of the interaction term becomes γ^2 , which is chosen to be very small, and thus, the interaction term can be made to blow up. In this way, the contribution to the energy of the interaction term can be made arbitrarily large, which we assume, and therefore, such a situation will be energetically disfavoured. What this means specifically is that the ϕ solitons may not pass through the ψ solitons (in which necessarily regions occur where the ψ field is significantly different for $\psi = \pm a$) without the energy blowing up. There is an energy barrier to such a process. Thus if ψ is forced to make a transition from $-a$ to a only before or after ϕ makes its transitions, the solitons of the ϕ field cannot pass through those of the ψ field without encountering an insurmountable energy barrier. But then the solitons of the ϕ field, the sheep, are trapped within the solitons of the ψ field, the shepherd.

Inside the domain wall, two adjacent ϕ half-solitons (say, one going from $\phi = 2k$ to $2k + 1$ and the other from $2k + 1$ to $2k + 2$) attract each other. This is because the energy is minimized by reducing the region over which ϕ is in its false vacuum, $\phi = 2k + 1$. Thus the net ϕ soliton passes from even integer to even integer. But then these full solitons further minimize their energy by separating as far as possible from each other, as this minimizes any gradient energies that occur due to their proximity; hence, they have a repulsive interaction. The half-solitons on either ends are also simply repelled by the adjacent full solitons.

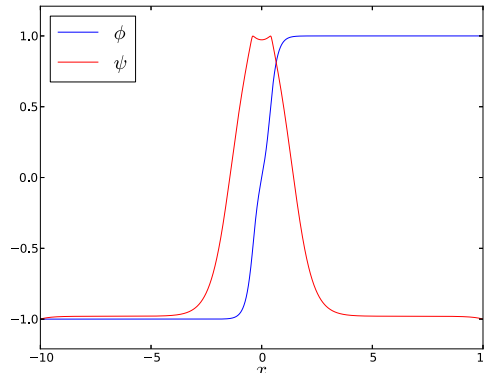


FIG. 4. The metastable domain wall configuration, ϕ passing from $-1 \rightarrow 1$ and ψ passing from $-1 \rightarrow 1 \rightarrow -1$. For this and all subsequent figures, the parameters were chosen as $a = 1$, $\epsilon_\phi = 0.01$, $\epsilon_\psi = 0.5$, $\lambda = 0.1$, $\alpha = 0.5$, $\beta = 0.5$, $\gamma = 0.01$.

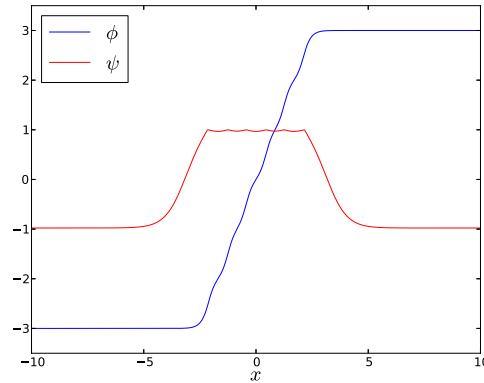


FIG. 5. The metastable domain wall configuration, ϕ passing from $-3 \rightarrow 3$ and ψ passing from $-1 \rightarrow 1 \rightarrow -1$.

Thus in the example shown in Figure 5, in which ϕ interpolates from -3 to $+3$, the half-soliton from -3 to -2 is repelled by the full soliton from -2 to 0 , which also repels the subsequent full soliton from 0 to $+2$ which in turn repels the final half-soliton from $+2$ to $+3$. The ψ (shepherd) solitons have the false vacuum $\psi \approx a$ in between them, so they attract one another. The sheep want to separate as far as possible from one another, but they cannot do so without pushing the shepherd solitons further and further apart. The energy in doing so increases linearly with the separation of the shepherd solitons. The competing energy decrease coming from the separating sheep is at best decreased to a constant value (the total mass of sheep) as the separation between the sheep becomes large. Hence, energetically, the shepherd solitons force the sheep solitons to be herded together at a finite size where the outward pressure from the sheep is balanced against the inward vacuum pressure pushing the shepherds together. The whole system forms a classically stable configuration. An even more extreme example is given in Figure 6 and the corresponding zooms in Figure 7, which contains 31 sheep.

However, quantum mechanically, the herded sheep are actually in a metastable configuration. Tunnelling processes can permit the ψ field to make a quantum transition to its true vacuum at all points where the ϕ field is near its true vacuum (and specifically away from values where $V(\phi) = V(1/2)$). Such transitions truly liberate the sheep, which can after the tunnelling transition move apart freely.

III. ANALYTICAL CALCULATION OF THE DECAY RATE IN THE FREE KINK APPROXIMATION

As we have just noted, the soliton is metastable: it will decay via quantum tunnelling. The tunnelling transition is mediated by an instanton, which is called a bounce. The bounce corresponds

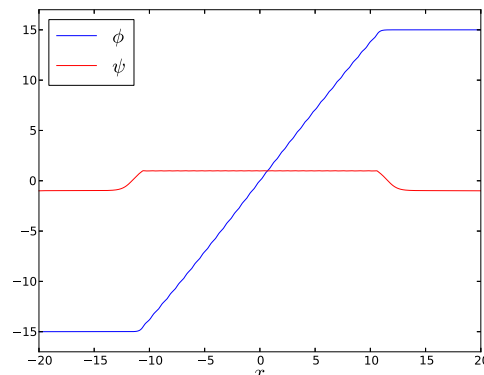


FIG. 6. The metastable domain wall configuration with 31 sheep, ϕ passing from $-15 \rightarrow 15$ and ψ passing from $-1 \rightarrow 1 \rightarrow -1$.

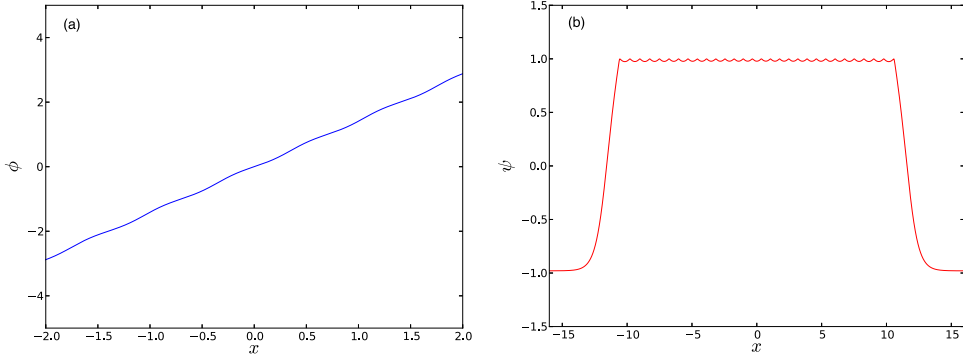


FIG. 7. (a) Zoom of the metastable domain wall configuration with 31 sheep for the field ϕ . (b) Zoom of the metastable domain wall configuration with 31 sheep for the field ψ .

to a trajectory in Euclidean time, $t \rightarrow -i\tau$. This changes the sign of the kinetic energy, $T \rightarrow -T$, and therefore, bounce configuration can be thought of as motion in the potential $-V$ where we include the spatial gradient terms as part of the potential. The Euclidean action can be written as $S_E = T + V$ and the conserved Euclidean “energy” is $E = T - V$. The bounce begins at the metastable configuration, arrives at the configuration which will materialize upon the event of the quantum transition, and then “bounces back,” that is, returns to the initial configuration. Therefore, the bounce will begin at the metastable soliton as in Fig. 8(a) followed by an evolution during which the field ψ which is initially equal to a in the region in between the two half-solitons sinks down until it finally makes it to $\psi = -a$, corresponding to a configuration of two free half-solitons as depicted in Fig. 8(b). The two half-solitons must be created, however, with some kinetic energy, since during the Euclidean evolution, the “energy” $T - V$ is conserved, and $-V$ is more negative at this configuration of two essentially free solitons. The solitons will then separate and rise up the (negative) potential until they stop, after which they bounce back. When they reach the bounce point, that is, the configuration at which they will materialize when the quantum tunnelling transition occurs, and from that point on, Minkowski evolution takes over.

The Euclidean Lagrangian is given by

$$L_E = \int dx \left(\frac{1}{2} \dot{\phi}^2 + \frac{1}{2} \dot{\psi}^2 + \frac{1}{2} \phi'^2 + \frac{1}{2} \psi'^2 + V(\phi, \psi) \right). \quad (7)$$

The fields depend on time only through their dependence on the positions of the solitons. Indeed, in a first approximation, the fields depend independently on the positions of the solitons, which is the appropriate collective coordinate describing their evolution. This means that we can approximate $\phi(x, \xi_1, \xi_2) = \phi_1(x - \xi_1) + \phi_2(x - \xi_2) + \phi_0$ while $\psi(x, \xi_1, \xi_2) = \psi_1(x - \xi_1) + \psi_2(x - \xi_2) + \psi_0$, where ϕ_0 and ψ_0 are necessary constant offsets. This approximation is certainly valid when the solitons are separated from one another. It is not valid when they are very close, and we will have to resort to numerical/approximate calculations to find the action there, but we leave that for later. For example, for $\dot{\psi}$ we get

$$\begin{aligned} \dot{\psi} &= \partial_{\xi_1} \psi(x, \xi_1, \xi_2) \dot{\xi}_1 + \partial_{\xi_2} \psi(x, \xi_1, \xi_2) \dot{\xi}_2 \\ &= \partial_{\xi_1} \psi_1(x - \xi_1) \dot{\xi}_1 + \partial_{\xi_2} \psi_2(x - \xi_2) \dot{\xi}_2 \\ &= -\partial_x \psi_1(x - \xi_1) \dot{\xi}_1 - \partial_x \psi_2(x - \xi_2) \dot{\xi}_2. \end{aligned} \quad (8)$$

$\partial_x \psi_1(x - \xi_1) = \psi'_1$ is a function that is sharply peaked around ξ_1 while $\partial_x \psi_2(x - \xi_2) = \psi'_2$ is sharply peaked around ξ_2 ; thus, the product of these functions essentially vanishes. This gives

$$L_E = \int dx \left(\frac{1}{2} \phi_1'^2 \dot{\xi}_1^2 + \frac{1}{2} \phi_2'^2 \dot{\xi}_2^2 + \frac{1}{2} \psi_1'^2 \dot{\xi}_1^2 + \frac{1}{2} \psi_2'^2 \dot{\xi}_2^2 + \frac{1}{2} (\phi_1'^2 + \phi_2'^2 + \psi_1'^2 + \psi_2'^2) + V(\phi, \psi) \right). \quad (9)$$

Furthermore, the nature of the solitons at ξ_1 and ξ_2 in each field is essentially identical: they are simply the “kink”-type solitons of an (almost) doubly degenerate (actually multiply degenerate, but

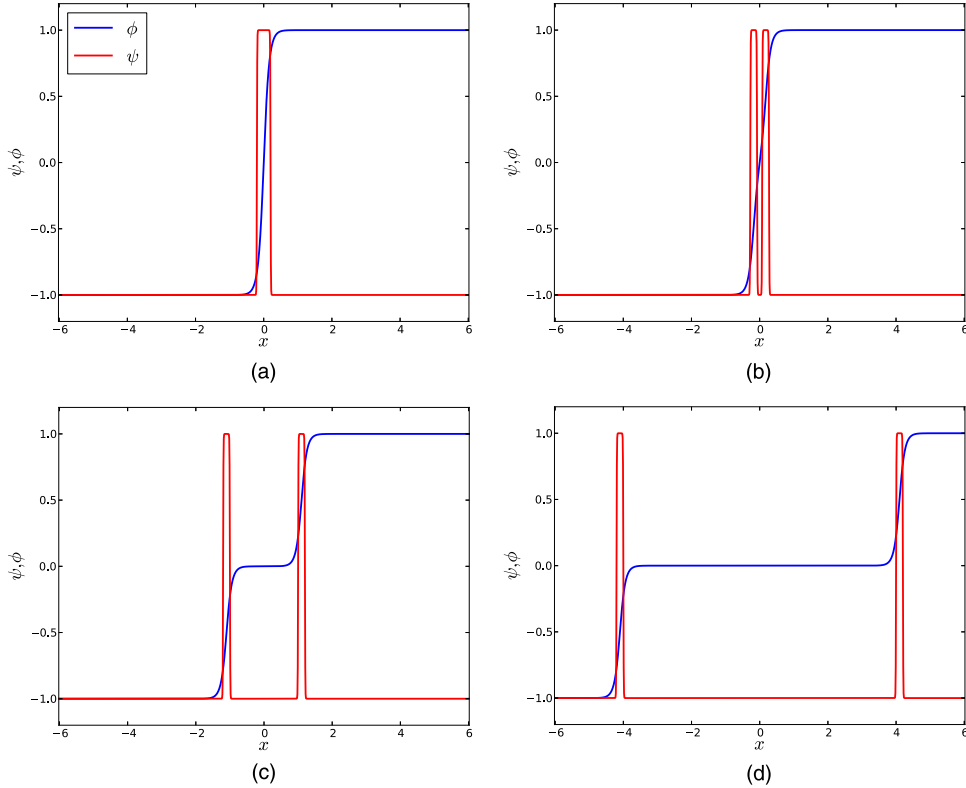


FIG. 8. (a) Metastable soliton configuration ($\xi=0$). (b) Solitons just touching ($\xi=0.15$). (c) Solitons separated by a macroscopic amount ($\xi=2$). (d) Solitons separated by a macroscopic amount ($\xi=8$). Here, we used parametrization (28) of the bounce trajectory with $a=1, \omega=10, \Omega=100$.

only adjacent minima are relevant here) potential. Therefore we will compute the contribution of the kinks in the limit that the potential is exactly degenerate, and we note that kink or antikink obviously gives an equal contribution. Thus we write

$$\int dx \frac{1}{2} \phi_1'^2 = \int dx \frac{1}{2} \phi_2'^2 \equiv \frac{m_\phi}{2} \quad \text{and} \quad \int dx \frac{1}{2} \psi_1'^2 = \int dx \frac{1}{2} \psi_2'^2 \equiv \frac{m_\psi}{2}. \quad (10)$$

m_ϕ and m_ψ should not be confused with the actual masses of the perturbative excitations of each respective field. The contribution of the potential to the action can also be easily deconstructed. There will be a contribution from around the region of each soliton and there will be a contribution from the region in between the solitons when they separate. We find that the interaction potential plays no role in evaluating the action. We will assume this for the moment and discuss it in more detail in Subsection III C.

A. Free kink approximation

We can write

$$\int dx V(\phi, \psi) \approx \int_{x \approx \xi_1} dx (V_\phi + V_\psi) + \int_{x \approx \xi_2} dx (V_\phi + V_\psi) \quad (11)$$

and we will compute each term in (10) and (11) in the free kink approximation. For a field χ , which satisfies an equation with solution given by a free kink, we have a Lagrangian

$$L = \frac{1}{2} \chi'^2 + V(\chi) \quad (12)$$

and equation of motion

$$\chi'' - V'(\chi) = 0. \quad (13)$$

The first integral of the equation of motion is conservation of energy,

$$\frac{1}{2}\chi'^2 - V(\chi) = C \rightarrow 0, \quad (14)$$

where C is a constant which we normalize to zero. Therefore $\chi' = \sqrt{2V(\chi)}$. Then the integrals that appear in the action above are reduced to quadrature

$$\int_{x_i}^{x_f} dx \frac{1}{2}\chi'^2 = \int_{x_i}^{x_f} dx \frac{1}{2}\sqrt{2V(\chi)}\chi' = \int_{x_i}^{x_f} d\chi \sqrt{\frac{V(\chi)}{2}} \quad (15)$$

and

$$\int_{x_i}^{x_f} dx V(\chi) = \int_{x_i}^{x_f} dx \frac{1}{2}\sqrt{2V(\chi)}\chi' = \int_{x_i}^{x_f} d\chi \sqrt{\frac{V(\chi)}{2}}, \quad (16)$$

evidently, the integrals are equal.

B. Analytical evaluation of the Euclidean action

For ϕ , the potential is $V_\phi = \alpha \sin^2(\pi\phi)$ which gives

$$\frac{m_\phi}{2} = \int_{x_i}^{x_f} dx \frac{1}{2}\phi'^2 = \int_{x_i}^{x_f} dx V_\phi(\phi) = \sqrt{\frac{\alpha}{2}} \int_{-1}^0 d\phi (-\sin(\pi\phi)) = \sqrt{\frac{\alpha}{2}} \frac{\cos(\pi\phi)}{\pi} \Big|_{-1}^0 = \frac{\sqrt{2\alpha}}{\pi}. \quad (17)$$

The minus sign in front of the $\sin(\pi\phi)$ comes from the square root since for the first kink $\phi \in [-1, 0]$ where $\sin(\pi\phi) \leq 0$. For the field ψ we have $V_\psi = \beta(\psi^2 - a^2)^2$ which gives

$$\frac{m_\psi}{2} = \int_{x_i}^{x_f} dx \frac{1}{2}\psi'^2 = \int_{x_i}^{x_f} dx V_\psi(\psi) = \sqrt{\frac{\beta}{2}} \int_{-a}^a d\psi (a^2 - \psi^2) = \frac{2}{3}\sqrt{2\beta}a^3. \quad (18)$$

We note the sign change in the intermediate equation as $(\psi^2 - a^2)$ is negative for $\psi \in [-a, a]$ and the limits x_i and x_f are assumed to be both close to ξ_1 or ξ_2 as required.

We will evaluate the energy, first in the metastable configuration and second in the configuration at the top of the potential barrier, so that eventually we can normalize the Euclidean action properly and then evaluate it. For the metastable configuration, the energy essentially obtains contributions from the locations of the kink solitons, two for ϕ and two for ψ , hence

$$\begin{aligned} E_0 &= \frac{1}{2} \int dx (\phi_1'^2 + \phi_2'^2 + \psi_1'^2 + \psi_2'^2) + \int_{\substack{x \approx \xi_1 \\ x \approx \xi_2}} dx V(\phi, \psi) \\ &= (m_\phi + m_\psi) + \int_{x \approx \xi_1} dx (V(\phi) + V(\psi)) + \int_{x \approx \xi_2} dx (V(\phi) + V(\psi)) \\ &= 2(m_\phi + m_\psi) \end{aligned} \quad (19)$$

using (17) and (18). We will subtract E_0 from the potential so that we normalize the initial configuration to vanishing energy.

For the configuration at the top of the potential barrier, which is actually at the bottom of a potential well since we invert the potential in the Euclidean dynamics, we must take into account the following differences: the solitons must have kinetic energy in order to conserve energy, we have two additional kinks in the ψ field, and if the solitons separate by a distance $|\xi_2 - \xi_1|$ the energy increases by $\int_{\xi_1}^{\xi_2} dx V(\phi, \psi)$. For the metastable configuration, we did not imagine that the solitons can separate; it is assumed that they are herded together by the shepherd field. If the solitons at the top of the potential barrier separate, they leave behind the true vacuum. Since we will normalize the vacuum energy so that the false vacuum outside the shepherd-sheep soliton has zero energy density, the true vacuum of the ϕ field between two sheep will have negative energy, so this contribution in

fact increases the energy in the Euclidean dynamics. The ψ field is in its true vacuum outside the shepherd soliton; thus there is no energy density difference for it. However, the ϕ field is in its false vacuum outside the shepherd soliton; hence, looking at potential (4), we see that the contribution will be

$$\int_{\xi_1}^{\xi_2} dx V(\phi, \psi) = -\alpha \epsilon_\phi |\xi_2 - \xi_1|. \quad (20)$$

Then the energy for the configuration at the top of the barrier will be

$$\begin{aligned} E_T - E_0 &= \frac{1}{2}(m_\phi + 2m_\psi)(\dot{\xi}_1^2 + \dot{\xi}_2^2) + 2(m_\phi + 2m_\psi) - 2(m_\phi + m_\psi) - \alpha \epsilon_\phi |\xi_2 - \xi_1| \\ &= \frac{1}{2}(m_\phi + 2m_\psi)(\dot{\xi}_1^2 + \dot{\xi}_2^2) + 2m_\psi - \alpha \epsilon_\phi |\xi_2 - \xi_1| \\ &= T + V. \end{aligned} \quad (21)$$

The Minkowski action is $S_M = \int dt (T - V)$ while the energy is $E = T + V$. Analytically continuing to Euclidean time, $T \rightarrow -T$ and $S_M \rightarrow -\int d\tau (T + V) = -S_E$. Then the Euclidean action is $S_E = \int d\tau (T + V)$ and is easily read off as

$$S_E = \int d\tau \left(\frac{1}{2}(m_\phi + 2m_\psi)(\dot{\xi}_1^2 + \dot{\xi}_2^2) + 2m_\psi - \alpha \epsilon_\phi |\xi_2 - \xi_1| \right), \quad (22)$$

where the overdot now means the derivative with respect to τ . The Euclidean trajectory, which we can compute analytically, starts at the configuration at the top of the barrier. The solitons separate until they reach the bounce point, and then they come back together and coalesce. We define center of mass and relative coordinates $X = (\xi_1 + \xi_2)/2$ and $\xi = \xi_2 - \xi_1$; in terms of these, $\dot{\xi}_1^2 + \dot{\xi}_2^2 = 2\dot{X}^2 + \frac{1}{2}\dot{\xi}^2$. We take the center of mass coordinate to be constant, $X = \dot{X} = 0$ so that $\dot{\xi}_1^2 + \dot{\xi}_2^2 = \frac{1}{2}\dot{\xi}^2$. The Euclidean ‘‘energy,’’ $T - V$, is conserved and normalized to zero

$$0 = T - V = \frac{1}{2} \left(\frac{m_\phi}{2} + m_\psi \right) \dot{\xi}^2 - 2m_\psi + \alpha \epsilon_\phi \xi, \quad (23)$$

where we restrict $\xi > 0$. The solitons separate until $\dot{\xi} = 0$, hence at that point which corresponds to the bounce point, $\xi = \xi_B$ which is given by

$$\xi_B = \frac{2m_\psi}{\alpha \epsilon_\phi}. \quad (24)$$

Then the contribution to the action from this part of the trajectory will be

$$S_E = \int d\tau \frac{1}{2} \left(\frac{m_\phi}{2} + m_\psi \right) \dot{\xi}^2 + 2m_\psi - \alpha \epsilon_\phi |\xi|. \quad (25)$$

Energy condition (23) implies

$$\dot{\xi} = 2\sqrt{\frac{(2m_\psi - \alpha \epsilon_\phi \xi)}{m_\phi + 2m_\psi}}. \quad (26)$$

Replacing in the usual way as in (12)-(16) for $\dot{\xi}$ in the first term of (25) we find

$$\begin{aligned} S_E &= \int d\tau \frac{1}{2} \left(\frac{m_\phi}{2} + m_\psi \right) 2\sqrt{\frac{(2m_\psi - \alpha \epsilon_\phi \xi)}{m_\phi + 2m_\psi}} \dot{\xi} + \sqrt{2m_\psi - \alpha \epsilon_\phi \xi} \frac{1}{2} \sqrt{m_\phi + 2m_\psi} \dot{\xi} \\ &= \int d\tau \sqrt{2m_\psi - \alpha \epsilon_\phi \xi} \sqrt{m_\phi + 2m_\psi} \dot{\xi} \\ &= \int_{\xi_T}^{\xi_B} d\xi \sqrt{2m_\psi - \alpha \epsilon_\phi \xi} \sqrt{m_\phi + 2m_\psi} = \frac{-2\sqrt{m_\phi + 2m_\psi} (2m_\psi - \alpha \epsilon_\phi \xi)^{3/2}}{3\alpha \epsilon_\phi} \Big|_{\xi_T \approx 0}^{\xi_B} \\ &= \frac{2\sqrt{m_\phi + 2m_\psi} (2m_\psi)^{3/2}}{3\alpha \epsilon_\phi}, \end{aligned} \quad (27)$$

where ξ_T is the value of ξ at the top of the barrier, which is of the order of the size of the solitons, but we can approximate it as zero. This is the contribution to the action of the part of the instanton from the top of the barrier to the bounce point.

C. Contribution of the interaction potential

In this subsection we give an argument why the interaction potential $V_{\phi\psi}$ does not contribute significantly to the energy and the action. If we imagine the sheep solitons separating, then between them the ϕ field will be in its true vacuum but the ψ field will be in its false vacuum. Thus as they separate, the total energy will grow linearly. Thus the shepherd solitons give a compression that holds the sheep together. However as the shepherd solitons compress the sheep more and more, there will be an increase in the pressure, and the system will come to an equilibrium. There are many contributions to the pressure forces, and the ϕ kinks becoming steeper than their natural slope will add energy and hence pressure. But there will be a contribution coming from the interaction term. Effectively the shepherd solitons would like to approach each other and annihilate completely in order to minimize their energy. The sheep solitons get in the way. The energy diminishes linearly as the separation of the shepherd solitons goes to zero, with coefficient $\beta\epsilon_\psi$. If one forces the shepherd solitons closer and closer, the value of the ψ field at the point where $\phi \approx 1/2$ starts to move significantly away from $\pm a$, the values for which the numerator of the interaction term vanishes. This will make the energy increase, to first approximation linearly, however with much greater coefficient $\kappa \gg \beta\epsilon_\psi$. Thus the dynamics can be simply modelled as given by an effective potential of the form

$$V_{\text{eff}} = \begin{cases} \beta\epsilon_\psi\xi & \text{for } \xi > \xi_0 \\ \beta\epsilon_\psi\xi - \kappa(\xi - \xi_0) & \text{for } \xi < \xi_0 \end{cases},$$

where the second term is valid only for $\xi \rightarrow \xi_0^-$ and ξ_0 is smaller than the size of the free solitons. For even smaller values of ξ , the repulsion quickly becomes large and quite non-linear. However, the energy in the compression term is comparable to $\beta\epsilon_\psi\xi_0$, which, along with the corresponding pressure, for small ϵ_ψ can be made very small. This compression will be balanced by an equal, and hence small, but opposing, repulsive force. Thus this contribution to the energy of the solitons is arbitrarily small in the limit $\epsilon_\psi \rightarrow 0$, which is what we assume. Therefore, we conclude that the interaction term does not contribute significantly to the energy of the solitons. The most physical analogy can be made to nuclei, which have intrinsic mass energy, proportional to the number of nucleons, but which is modified by the binding energy of the nucleons. For precision measurements the binding energies are important, but in the values of the overall masses, they are quite negligible.

D. Contribution of the trajectory from the initial metastable state to the top of the barrier

The Euclidean evolution from the initial metastable configuration corresponds to a complicated evolution until the system reaches a configuration at the point that we have called the top of the barrier. Although for the Euclidean time evolution which occurs in the inverted potential, a more accurate nomenclature for this point would be the ‘‘bottom of the well,’’ we will continue to call it the top of the barrier as that is what it is in the real time dynamics. The configuration at the top of the barrier corresponds to two distinct sheep and shepherd solitons that are separated by the minimal amount required so that there is no appreciable deformation of their profiles due to the interaction between them. The subsequent Euclidean evolution can be well approximated by the free kinks, which we can then treat analytically giving the contribution to the action in Eq. (27). In principle would have to resort to numerical methods to calculate the contribution to the action of the part of the trajectory from the initial configuration to the top of the barrier, however, in practice, we will be able to analytically compute an upper bound to it and then be able to conclude that it is negligible compared with contribution Eq. (27). With a simple parametrization of the configuration in terms of hyperbolic tangents, which are the free kinks of the $(\psi^2 - a^2)^2$ potential and inverse tangents of exponential argument, which are the free kinks of the sin-Gordon model, we can get this upper

bound of the contribution to the action from the initial part of the trajectory. Taking

$$\begin{aligned}\psi(x, \xi) &= a \left\{ \tanh \Omega(x + (\xi/2 + 2/\omega)) - \tanh \Omega(x - (\xi/2 + 2/\omega)) \right. \\ &\quad \left. - \left(\tanh \Omega(x + \xi/2) - \tanh \Omega(x - \xi/2) \right) - 1 \right\}, \\ \phi(x, \xi) &= \frac{2}{\pi} \left\{ \tan^{-1} e^{\omega(x + (\xi/2 + 1/\omega))} + \tan^{-1} e^{\omega(x - (\xi/2 + 1/\omega))} \right\} - 1,\end{aligned}\quad (28)$$

where $\Omega = \sqrt{2\beta}a$ and $\omega = \sqrt{2\alpha}\pi$, while ξ is the separation parameter, this function is depicted in Figs. 8(a)–8(d).

The numerically evaluated effective potential for parametrization (28) is shown in Figure 9. The actual exact instanton trajectory may involve very much more complicated configurations, such as exciting shape deformations, breather modes, and radiating waves; however, the exact trajectory will give the minimum value for the Euclidean action. Therefore any value that we compute using the explicit parametrization of Eq. (28) will simply give an upper bound for the action, and subsequently a lower bound for the decay rate. We will find that the upper bound that we obtain for the contribution to the action from the initial part of the instanton trajectory is in fact negligible in comparison to the contribution from the remainder of the trajectory, where the two solitons separate, reach the turning point, and bounce back, computed in Eq. (27). The behaviour of the potential for separation of the solitons greater than their intrinsic size is completely understandable in terms of the energy found in (21), which corresponds to the part of the potential starting at the top of the barrier and descending along a very slightly sloped straight line. The bounce point is achieved at $\xi_B = 2m_\psi/\alpha\epsilon_\phi$, which obviously behaves as $o(1/\epsilon_\phi)$. The trajectory from the initial metastable state to the top of the barrier, in the parametrized set of configurations of Eq. (28), achieves the top of the barrier with ξ varying from 0 to $\approx 4/\Omega$, starting from where the two ϕ solitons are just touching each other and there are no ψ solitons between them to a separation of the order of the width of the two ψ solitons that subsequently appear between the two ϕ solitons. We emphasize that this is a size which is $o(1)$ when compared with $o(1/\epsilon_\phi)$. The Euclidean action, for the parametrized configuration can be evaluated analytically or numerically, we will be content with a combination of the two. Compared to the evaluation in Eq. (27) the following complication arises. The ψ solitons between the two sheep solitons are not initially well separated, hence the arguments given after Eq. (8) are not valid. But we can easily calculate the action explicitly and we find

$$\begin{aligned}S_E &= \int d\tau dx \left(\frac{1}{2} (\partial_\xi \phi^2 + \partial_\xi \psi^2) \dot{\xi}^2 + \frac{1}{2} (\phi'^2 + \psi'^2) + V(\phi, \psi) \right) \\ &= \int d\tau \left(\frac{1}{2} M(\xi) \dot{\xi}^2 + V_{\text{eff.}}(\xi) \right),\end{aligned}\quad (29)$$

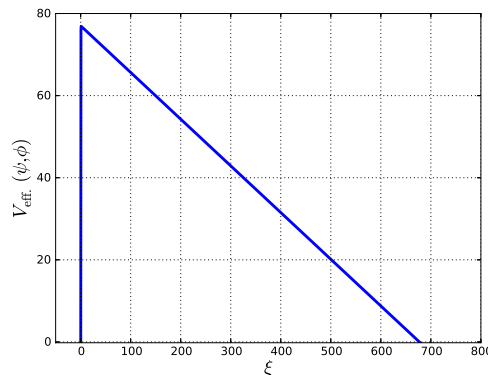


FIG. 9. Potential $V_{\text{eff.}}(\xi)$ for parametrization (28) of the bounce trajectory with the same parameter choice as in Fig. 8. We have checked that the potential is perfectly smooth at the top of the barrier. The parameters are chosen as $a = 30$, $\alpha = \beta = 5$, $\Omega = 94.86$, $\omega = 9.93$, $\gamma = 0.01$, $\lambda = 0.1$, $\epsilon_\phi = 0.01$, $\epsilon_\psi = 0.5$.

where

$$M(\xi) = \frac{\omega}{\pi^2} + 2a^2\Omega \left(\frac{1}{3} + (\xi \coth(\xi) - 1)\text{csch}^2(\xi) + \frac{1}{3} \right) \quad (30)$$

is now a ξ dependent mass and $V_{\text{eff.}}(\xi)$ is evaluated numerically and is shown in Fig. 9. It is of course completely possible to evaluate $V_{\text{eff.}}(\xi)$ analytically, but this does not shed any more light on the situation. The potential rises robustly to the top of the barrier, what we have calculated approximately as $2m_\psi$ in Eq. (21). Most importantly, there are only minor, perturbative corrections in ϵ_ϕ or ϵ_ψ , which we can obviously neglect in lowest approximation. The ξ dependent mass is a smooth function of ξ , which is maximal at $\xi = 0$ and quickly achieves a constant asymptotic value as ξ increases. Action Eq. (29) being independent of Euclidean time gives equations of motion that conserve “energy” and hence admits a first integral even though the mass depends on ξ ,

$$\frac{1}{2}M(\xi)\dot{\xi}^2 - V_{\text{eff.}}(\xi) = 0. \quad (31)$$

Then using the by now familiar procedure, we obtain

$$S_E = \int_0^{\xi \approx (2/\Omega)} d\xi \sqrt{2M(\xi)V_{\text{eff.}}(\xi)} \sim o(1). \quad (32)$$

Thus we conclude that the contribution to the action from the initial part of the bounce configuration is at most of $o(1)$, and comparing with the contribution to the action from the remainder of the bounce trajectory, Eq. (27) which is of $o(1/\epsilon_\phi)$, it is perfectly reasonable to neglect this contribution to the Euclidean action.

IV. DISCUSSION

We have computed the decay of a domain wall which traps the true vacuum inside the false vacuum. At first glance, one would think that such a domain wall would be classically unstable to dissociation; however, it is easy to conceive of interactions which keep the soliton classically stable. The model presented here may be artificial; however, the general idea is clear. Any potential which prevents the passage of the sheep solitons through the shepherd solitons will do.

There is furthermore no analogous surface energy that occurs in two^{6,7} and three⁸ spatial dimensional examples, which could trap the true vacuum inside, at least classically. However, in this paper we find that we can build on the analogy with the two spatial dimensional models.^{6,7} In those models, the true vacuum was separated from the false vacuum by a thin wall. The thin wall was achieved by having several topological quanta of one of the fields trapped inside the wall. The pressure of these quanta made the wall thin. It may well be that the thin wall monopole suggested in Ref. 8 in fact only occurs for large monopole charge as has been found in several large charged BPS monopoles.⁹

In the present paper, we also trap N solitons of the field ϕ inside the confining soliton of the field ψ . The N solitons in principle exert a pressure and the overall size of the full soliton is proportional to N . The decay of the soliton can occur through tunnelling transitions. In the initial metastable configuration, the external false vacuum is due to the ϕ field; the ψ field is in its true vacuum. However, inside, the ψ field goes to its false vacuum while the ϕ field interpolates from the false vacuum to the true vacuum and back to the false vacuum multiple times, finally exiting the confining region in its false vacuum. Tunnelling transitions, essentially in the field ψ inside the confining soliton, will cut the soliton into two parts. The region between the two parts is in the true vacuum for both fields. This could happen at any point within the confining soliton where the ϕ field crosses its true vacuum, which occurs multiple times if there are multiple ϕ solitons confined. It will continue to occur until all the ϕ solitons are free. The configuration will then resemble one half-soliton, linking the false vacuum on the outside to the true vacuum, followed by a string N of full solitons, in which the ϕ field makes the transit from true to adjacent false to the subsequent true vacua while the ψ field makes the transition true to false and back to true vacua, followed by a final half-soliton interpolating from the true vacuum to the false vacuum on the outside at the other end.

However, after any one transition, the false vacuum outside will be unstable to the groups of herded solitons from separating apart, converting false vacuum to true vacuum. We have computed the decay rate for the “fundamental” meta-stable soliton consisting of a bound state of two half-solitons, where the ϕ field goes only once, from false vacuum to true vacuum to false vacuum. The decay rate is proportional to

$$\Gamma \sim e^{-2\sqrt{m_\phi+2m_\psi}(2m_\psi)^{3/2}/3\alpha\epsilon_\phi} K, \quad (33)$$

where K is the usual determinant prefactor.^{10,11} We note that parametrically for α large enough, this decay rate can be unsuppressed.

The decay rate for each tunnelling transition for the decay on N herded sheep must be calculated separately for each process, by essentially the same methods as we have done above. The calculation of the effective potential is essentially identical to our analysis, and only the zero of the energy has to be defined corresponding to the original N sheep meta-stable soliton. The inertia terms will however be different. The masses of the daughter solitons formed after the decay process depend on where the ψ field makes its transition to its true minimum and cuts the original soliton into two pieces. In general they will be different from the masses that we have calculated Eqs. (17) and (18), and this will affect the value of the euclidean action for the tunnelling process. The calculation is straightforward and left to the reader, we do not expect any surprises.

ACKNOWLEDGMENTS

We thank NSERC of Canada for financial support. We thank St. John’s College and DAMTP, both of Cambridge University for hospitality, where this work was completed. Some of the work of M.H. was undertaken at DAMTP University of Cambridge, financially supported by the UK Science and Technology Facilities Council under Grant No. ST/J000434/1. We thank Nick Manton for useful discussions. M.H. would also like to thank Jennifer Ashcroft for helpful comments.

¹ M. Shifman, *Advanced Topics in Quantum Field Theory: A Lecture Course* (University Press, Cambridge, UK, 2012); A. Vilenkin, *Phys. Rep.* **121**, 263 (1985).

² J. Braden, J. R. Bond, and L. Mersini-Houghton, *J. Cosmol. Astropart. Phys.* **1503**(03), 007 (2015).

³ P. M. Chaikin and T. C. Lubensky, *The Principles of Condensed Matter Physics* (Cambridge University Press, Cullity, 1995); C. D. Graham, *Introduction to Magnetic Materials*, 2nd ed. (Wiley IEEE, New York, 2008); E. K. H. Salje, *Phase Transitions in Ferroelastic and Co-elastic Crystals* (Cambridge University Press, Cambridge, 1993).

⁴ É. Dupuis, Y. Gobeil, R. MacKenzie, L. Marleau, M. B. Paranjape, and Y. Ung, *Phys. Rev. D* **92**, 025031 (2015).

⁵ J. P. Vial and I. Zang, *Math. Oper. Res.* **2**, 253 (1977); W. H. Press, S. A. Teukolsky, W. T. Vetterling, and B. P. Flannery, *Numerical Recipes in FORTRAN: The Art of Scientific Computing* (Cambridge University Press, 1992), ISBN: 9780521430647.

⁶ B. H. Lee, W. Lee, R. MacKenzie, M. B. Paranjape, U. A. Yajnik, and D. h. Yeom, *Phys. Rev. D* **88**, 085031 (2013).

⁷ B. H. Lee, W. Lee, R. MacKenzie, M. B. Paranjape, U. A. Yajnik, and D. h. Yeom, *Phys. Rev. D* **88**(10), 105008 (2013).

⁸ B. Kumar, M. B. Paranjape, and U. A. Yajnik, *Phys. Rev. D* **82**, 025022 (2010).

⁹ S. Bolognesi, *Nucl. Phys. B* **752**, 93 (2006); N. S. Manton, *Phys. Rev. D* **85**, 045022 (2012).

¹⁰ S. R. Coleman, *Phys. Rev. D* **15**, 2929 (1977).

¹¹ C. G. Callan, Jr. and S. R. Coleman, *Phys. Rev. D* **16**, 1762 (1977).